A NOVEL DIFFUSION FILTER FOR IMAGE RESTORATION AND ENHANCEMENT

ROMULUS TEREBES[1], MONICA BORDA[1], SORIN POP[1], OLIVIER LAVIALLE[2], CHRISTIAN GERMAIN[2], COSMIN LUDUŞAN[1,2]

Key words: Diffusion processes, Image restoration, Image orientation analysis.

We are proposing a new filter for image restoration and enhancement tasks that relies on image orientation analysis techniques for steering and directing smoothing or enhancement processes. The filter is developed under the Partial Differential Equations (PDE) framework using asymmetric orientation estimation operators and it has better junction preservation and noise removal properties than existing classical PDE based methods. We employ an experimental setup involving several computer generated images and a statistical interpretation of the results for proving the efficiency of the method in processing images composed of directional textures and degraded by additive Gaussian noise. The algorithm is compared also with state–of-the-art non-PDE based methods in filtering images containing oriented patterns.

1. INTRODUCTION

Within the PDE framework an image restoration or enhancement process is modeled using a continuous equation with theoretical properties allowing handling a particular degradation model. The simplest PDE is the isotropic diffusion equation; for a gray scale image modeled through a luminance function $U(x,y)$, the associated PDE is defined as follows:

$$\frac{\partial U}{\partial t} = \operatorname{div}(c\nabla \boldsymbol{U}). \tag{1}$$

It has been shown that, for constant diffusivities c, this linear filter is equivalent to a convolution of the input image with a bi-dimensional Gaussian kernel with a given standard deviation. Consequently, the solution of the PDE, computed for a given observation scale t, is blurry and does not allow edge preservation. Perona and Malik [1] were the first to address this issue by proposing a diffusion filter that penalizes diffusion between regions separated by gradient vector norms $|\nabla \boldsymbol{U}|$, superior to a threshold K. Their anisotropic diffusion PDE is governed by the same equation (1), endowed with a diffusivity function $g(.)$:

[1] Technical University of Cluj-Napoca, 15 C. Daicoviciu Street, Romulus.Terebes@com.utcluj.ro
[2] CNRS, IMS, UMR 5218, 351 Cours de la libération, 33405 Talence, France.

$$c \to g\left(\left|\nabla \mathbf{U}\right|\right) = \left[1 + \left(\left|\nabla \mathbf{U}\right| / K\right)^2\right]^{-1}. \tag{2}$$

The behavior of the filter can be more easily understood if the equation is put in terms of directional derivatives along axes collinear with vectors pointing in the structure directions ($\boldsymbol{\xi}$) and the orthogonal ones ($\boldsymbol{\eta}$):

$$\frac{\partial U}{\partial t} = c_\xi U_{\xi\xi} + c_\eta U_{\eta\eta}, \tag{3}$$

with:

$$\begin{cases} c_\xi = g\left(\left|\nabla \mathbf{U}\right|\right) \\ c_\eta = g\left(\left|\nabla \mathbf{U}\right|\right) + \left|\nabla \mathbf{U}\right| g'\left(\left|\nabla \mathbf{U}\right|\right). \end{cases} \tag{4}$$

Meanwhile the diffusion coefficient in the $\boldsymbol{\xi}$ direction is always positive, the one in the $\boldsymbol{\eta}$ direction becomes negative for gradient vector norms superior to K [1], the most important parameter of the method. On this direction the filter can invert the smoothing process leading to an edge enhancement action introducing (theoretically) unbounded oscillations. Edge enhancement is however deliberately introduced in the model since a maximum discrete principle can be imposed in the numeric domain by appropriate approximation schemes.

A relevant modification of the equation was introduced in a later publication by Catté *et al.* [2]; the authors show that a simple preconvolution with a Gaussian kernel of standard deviation $\sigma(G_\sigma)$ can be employed in order to avoid noise amplification and still allow edge enhancement to take place:

$$c \to g\left[\nabla\left(\left|G_\sigma * U\right|\right)\right] = g\left(\left|\nabla \mathbf{U}_\sigma\right|\right) = \left[1 + \left(\left|\nabla \mathbf{U}_\sigma\right| / K\right)^2\right]^{-1}. \tag{5}$$

A different approach was taken in [3–4] by Weickert in proposing tensor driven diffusion processes, expressed formally as follows:

$$\frac{\partial U}{\partial t} = \operatorname{div}\left[\left(\mathbf{v}^{\mathrm{T}} \mid \mathbf{u}^{\mathrm{T}}\right)\begin{pmatrix} g_1(\lambda_1,\lambda_2) & 0 \\ 0 & g_2(\lambda_1,\lambda_2) \end{pmatrix}\begin{pmatrix} \mathbf{v} \\ \mathbf{u} \end{pmatrix}\nabla \mathbf{U}\right]. \tag{6}$$

A popular choice falling into this category is the *Coherence Enhancing Diffusion* filter (CED) [3] and in this case the diffusion tensor $\boldsymbol{D}$ is derived from a set of eigenvectors computed using a structure tensor based approach. The two diffusivity functions $g_{1,2}(.,.)$ are dependent on the eigenvalues ($\lambda_{1,2}$) of the structure tensor and they are chosen in order to impose a specific action for the PDE. In the

case of the CED filter, a coherence measure is defined for favoring preferential smoothing along the structure directions (***u***) [3], computed as the orientation of the eigenvector corresponding to the smallest eigenvalue λ_2. The filter has been later adapted in order to better handle junctions and corners in [5].

Other authors considered also that semi-local orientation information must be used in order to obtain robust smoothing or enhancing directions. We only mention here the works of Carmona [6] and Tschumperlé [7–9], both being based on a direct formulation of a diffusion filter in terms of second order directional derivatives along the diffusion axes ***u*** and ***v***. For instance, the filter proposed in [7] computes the solutions of the following PDE:

$$\frac{\partial U}{\partial t} = \frac{1}{\left(\lambda_1 + \lambda_2 + 1\right)^{p_1}} U_{uu} + \frac{1}{\left(\lambda_1 + \lambda_2 + 1\right)^{p_2}} U_{vv} + \frac{2}{\pi} \nabla \mathbf{U}^t \int_{\alpha=0}^{\pi} \mathbf{J}_{\sqrt{T}a_\alpha} \sqrt{\mathbf{T}} a_\alpha \mathrm{d}\alpha \,, \tag{7}$$

where α is an orientation in the plane, $\boldsymbol{a}_\alpha = (\cos\alpha \sin\alpha)^t$, J is the Jacobian operator and T is a matrix obtained via a trace operation from the structure tensor. The first two terms represent a directional decomposition of a diffusion process and the last one is used in order to impose curvature preserving properties to the smoothing process. The parameters p_1 p_2 define the anisotropy of the smoothing process.

In [10] we introduced the following PDE filter:

$$\frac{\partial U}{\partial t} = \frac{\partial}{\partial u}\left[g(U_{\sigma_u}) U_u \right] + \frac{\partial}{\partial v}\left[g(U_{\sigma_u}) U_u \right], \tag{8}$$

with u and v denoting the coordinates along the eigenvectors of the structure tensor and $g(.)$ representing a Perona-Malik like diffusion function. The results included in [10] showed that the filter can preserve or enhance junctions and corners and has good noise removal properties.

2. PROPOSED METHOD

The improved filter is a derivation of the method in [10]. We propose a new formulation of the PDE that introduces asymmetry in the restoration process for directing it away from possible discontinuities of the luminance function such as corners and junctions. The filter is formulated both in the continuous and discrete domains in this section and its efficiency is proven statistically in section 3.

2.1. CONTINUOUS MODEL

Structure tensor based estimation operators are issuing an ambiguity in the definition of the diffusion axis due to the fact that the orientation of the underlying eigenvectors is computed using symmetric, modulo π, gradient information.

The fundamental idea behind the recently introduced asymmetric orientation estimation approaches [11–12] is to define the orientation of the underlying patterns at a semi-local scale in an asymmetrical manner *i.e.* on a modulo 2π per basis.

We employ for our new PDE-based filter the information provided by such an operator – IRON *(Isotropic Recursive Oriented Network)* – reported to be robust against additive Gaussian like noise in [12]. The operator introduces asymmetry in the orientation estimation process by using non-centered, sliding windows $W(x.y,\theta)$ on which the variance of the luminance function is computed. These windows are steered in each pixel (x_0, y_0) for all possible orientations $\theta \subset [0, 2\pi)$ and the orientation is defined as being the angle that corresponds to the maximal homogeneity *i.e.* the minimal variance [12].

Despite being computationally expensive, such an approach handles naturally discontinuities of the luminance function such as corners and junctions that are asymmetric by nature. In conjunction with PDE-based filters, IRON was previously used in [13] in a multi-directional diffusion model that uses a unique, initial orientation estimation step.

For including asymmetric orientation information in a PDE-driven iterative process, we assume right-side semi-differentiability on the maximum homogeneity axis on corners and junctions and differentiability on symmetric patterns and on the orthogonal directions. We propose the following filter integrating these constraints:

$$\begin{aligned}\frac{\partial U}{\partial t} = {} & 0.5\cdot[1-f(\frac{\partial_+ U}{\partial u},\frac{\partial_- U}{\partial u})]\frac{\partial_+}{\partial u}[g(U_{\sigma_u})U_u\,]+ \\ & +\max\left[0, f(\frac{\partial_+ U}{\partial u},\frac{\partial_- U}{\partial u})\right]\frac{\partial}{\partial u}[g(U_{\sigma_u})U_u]+\frac{\partial}{\partial v}[g(U_{\sigma_v})U_v]\end{aligned}, \tag{9}$$

with $\frac{\partial_\pm}{\partial u}$ denoting, respectively, the right and left one-sided derivatives along the positive and negative senses of the diffusion axis issued by an IRON operator.

The purpose of the function f is to detect possible asymmetric configurations along the structure's directions and, for this purpose, we employ a formulation inspired from the *minmod* function used in hyperbolic equations, that is able to detect any local extrema [16]:

$$f(a,b) = \mathrm{sgn}(a)\cdot\mathrm{sgn}(b). \tag{10}$$

Meanwhile, on symmetric differentiable patterns equation (9) is equivalent to (8), on discontinuities of the luminance function $(f(\frac{\partial_+ U}{\partial u},\frac{\partial_- U}{\partial u}) = -1)$ it can be expressed as follows:

$$\frac{\partial U}{\partial t} = \frac{\partial_+}{\partial u}\left[g(U_{\sigma_u})U_u \right] + \frac{\partial}{\partial v}\left[g(U_{\sigma_v})U_v \right]. \tag{11}$$

Equation (11) induces one-sided smoothing or enhancement processes in the maximum homogeneity direction computed by the IRON operator.

2.2. NUMERICAL APPROXIMATION SCHEME

The numerical approximation scheme was derived in order to transpose the properties of the continuous model using two-sided or one-sided finite differences operators, depending on the local structure of the processed image.

On symmetric patterns we employ a Perona-Malik like numerical scheme along the estimated directions [10, 16]:

$$\begin{aligned} \frac{\partial U}{\partial t} &= g[D_u^+(U_\sigma)]D_u^+(U) - g[D_u^-(U_\sigma)]D_u^-(U) + \\ &+ g[D_v^+(U_\sigma)]D_v^+(U) - g[D_v^-(U_\sigma)]D_v^-(U), \end{aligned} \tag{12}$$

with both backward and forward differences operators as numerical approximations of the directional derivatives :

$$\begin{cases} D_u^{\pm}(U) = \pm(U_{u\pm1,v} - U_{u,.v}) \\ D_v^{\pm}(U) = \pm(U_{u,v\pm1} - U_{u,.v}) \end{cases}. \tag{13}$$

On asymmetric patterns we assume only semi-differentiability on the ***u*** direction and we derive another numerical approximation scheme that accounts for this. We first approximate the right derivative by using one-sided Taylor series based development:

$$\frac{\partial_+}{\partial u}\left[g(U_{\sigma_u})U_u \right] \approx 2\left\{ \left[g(U_{\sigma_u})U_u \right]\Big|_{u+1/2,v} - g(U_{\sigma_u})U_u\Big|_{u,v} \right\}. \tag{14}$$

Equation (14) can be further expressed as follows:

$$\frac{\partial_+}{\partial u}\left[g(U_{\sigma_u})U_u \right] \approx 2\left\{ g(U_{\sigma_u})\Big|_{u+1/2,v} D_u^+(U) - g(U_{\sigma_u})U_u\Big|_{u,v} \right\}. \tag{15}$$

For approximating the diffusivity function with a sub-pixel resolution, we employ the same approach as Perona and Malik:

$$g(U_{\sigma_u})\Big|_{u+1/2,v} \approx g(U_{\sigma_u}\Big|_{u+1/2,v}) = g[D_u^+(U_\sigma)]. \tag{16}$$

The last term in equation (16) can be computed analytically for each pixel:

$$\frac{\partial U}{\partial t} = 2\Big\{g[D_u{}^+(U_\sigma)D_u{}^+(U) - g(U_{\sigma u})U_u\Big\} + \\ + g[D_v^+(U_\sigma)]D_v^+(U) - g[D_v^-(U_\sigma)]D_v^-(U) \quad (17)$$

The complete semi-discrete numerical model includes also an approximation for the asymmetry detector function *f*:

$$\frac{\partial U}{\partial t} = 0.5\cdot\Big\{1 - f[D_u^+(U), D_u^-(U)]\Big\}\cdot\Big\{g[D_u{}^+(U_\sigma)D_u{}^+(U)] - g(U_{\sigma u})U_u\Big\} + \\ + \max\Big[0, f[D_u^+(U), D_u^-(U]\Big]\cdot\Big\{g[D_u^+(U_\sigma)]D_u^+(U) - g[D_u^-(U_\sigma)]D_u^-(U)\Big\} + \\ + g[D_v^+(U_\sigma)]D_v^+(U) - g[D_v^-(U_\sigma)]D_v^-(U). \quad (18)$$

The time derivative is approximated by a forward finite difference and we use biquadratic interpolation to handle the needed sub-pixel precision [10].

3. RESULTS

Any attempt to compare PDE based filters is a difficult task. Most models have a large number of parameters and the quality of the filtered results depends strongly on the particular choice for this set. Having generated an original noise-free image and a degraded image, we opted for a full search in the parameter space in order to find the best filtered result that maximizes an objective measure. The experimental setup includes 15 computer generated images composed of random directional patterns, deliberately degraded by Gaussian noise; an example in shown in Fig. 1 and the obtained results are summarized in Table 1.

Based on recent developments in image quality assessment we used the variance weighted structural similarity index (VW-SSIM) [15] as the objective measure that is able to quantify the quality of the processed results in correspondence with the quality perceived by the human visual system. For further reference we also include in Table 2 the best peak signal-to-noise ratios (PSNR). All semi-local orientation driven methods yield better results than the anisotropic diffusion PDE and the proposed method is quantitatively superior.

In order to investigate if these results are due to the particular choice of the test images or if they are representative for the performances of a method, we performed a non-parametric two-way rank analysis of variance (ANOVA) [14] on the VW-SSIM measures; the results are shown in Table 2.

More that 90 % of the variability between the obtained VW-SSIM results is due to the processing method employed and to the nature of the processed image

itself. The two-way ANOVA design allows us to isolate and investigate only the method effect and the extremely low probability ($p = 2.48 \cdot 10^{-18}$) of a statistical Fisher-Snédécou test ($F = 52.6456$), indicates that the chosen processing method has a significant influence on the processed result.

Table 1

Quantitative measures. Best VW-SSIM and PSNR values for the experimental setup

Image	VW-SIM /*PSNR* degraded image		Best filtered results VW-SSIM /*PSNR* values									
			Catte et al. Eq.(1,5)		CED Eq.(6)		Tschumperle Deriche Eq.(7)		Symmetric PDE Eq.(8)		Asymmetric PDE Eq.(9)	
Method label			*CAT*		*CED*		*TSD*		*SYM*		*ASY*	
1	0.8881	*22.15*	0.9600	*28.03*	0.9767	*29.44*	0.9767	*29.40*	0.9835	*31.88*	**0.9876**	***32.66***
2	0.9242	*18.51*	0.9543	*21.85*	0.9724	*23.27*	0.9712	*23.24*	0.9795	*25.16*	**0.9809**	***25.21***
3	0.9009	*21.21*	0.9642	*26.35*	0.9756	*27.81*	0.9780	*28.16*	0.9827	*29.61*	**0.9850**	***29.80***
4	0.8581	*20.17*	0.9780	*29.11*	0.9675	*28.40*	0.9778	*28.21*	0.9844	*29.96*	**0.9867**	***30.72***
5	0.9102	*20.15*	0.9784	*26.85*	0.9790	*26.81*	0.9780	*26.50*	0.9831	*28.15*	**0.9837**	***28.30***
6	0.8535	*20.10*	0.9561	*26.35*	0.9637	*26.92*	0.9653	*26.87*	0.9737	*28.70*	**0.9777**	***28.98***
7	0.8068	*13.25*	0.9312	*19.19*	0.9595	*21.07*	0.9556	*20.78*	0.9637	*21.95*	**0.9649**	***22.17***
8	0.9019	*19.40*	0.9693	*24.95*	0.9749	*25.67*	0.9740	*25.54*	0.9812	*26.96*	**0.9833**	***27.20***
9	0.8885	*20.19*	0.9672	*25.71*	0.9690	*25.81*	0.9726	*26.09*	0.9784	*27.70*	**0.9810**	***28.27***
10	0.9523	*22.13*	0.9848	*27.44*	0.9850	*27.38*	0.9859	*27.52*	0.9894	*29.32*	**0.9894**	***29.41***
11	0.9031	*20.20*	0.9824	*28.08*	0.9809	*27.64*	0.9803	*27.60*	0.9861	*29.37*	**0.9883**	***29.98***
12	0.9222	*20.10*	0.9673	*24.52*	0.9766	*25.71*	0.9744	*25.43*	0.9833	*27.44*	**0.9834**	***27.45***
13	0.9462	*22.09*	0.9825	*27.50*	0.9854	*27.98*	0.9847	*27.74*	0.9861	*30.30*	**0.9900**	***30.51***
14	0.9211	*22.04*	0.9781	*27.24*	0.9791	*28.35*	0.9821	*28.09*	0.9867	*29.71*	**0.9883**	***29.87***
15	0.9061	*21.21*	0.9657	*28.41*	0.9759	*28.08*	0.9751	*28.73*	0.9810	*30.76*	**0.9820**	***31.09***

Table 2

Non-parametric ANOVA performed on the values in table 1

Source of variance	Sum of squares	Degrees of freedom	Mean square	F	p
Total	35,150	74	475		
Between images	19,934	14	1424		
Between methods	12,020	4	3005	52.65	2.45E-18
Residual	3,196	56	57		

The ANOVA's residual allows us to perform a post-hoc, multiple mean comparison test for further classifying the results. The mean ranks computed for each method over the 75 VW-SSIM measurements included in Table 1, are: $R_{CAT} = 23.07$, $R_{CED} = 29.80$, $R_{TSC} = 31.20$, $R_{SYM} = 50.07$, $R_{ASY} = 55.87$. A classical Bonferroni statistical test, computed at a 0.05 level of significance, yields a critical value for the multiple means comparison test equal to 5.52 and we may thus conclude that the proposed method outperforms all the other considered methods.

The correspondence between the VW-SSIM measure and the visual quality of the results is shown in Fig. 1 for an image included in the experimental set.

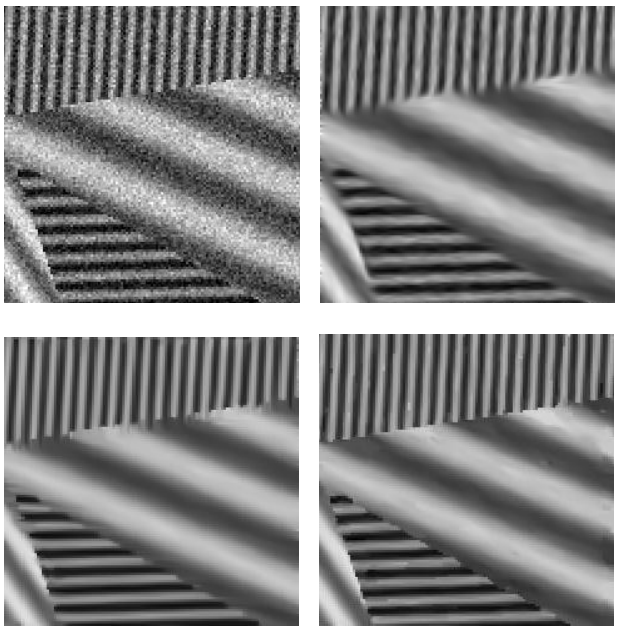

Fig. 1 – Results on computer generated images. First line, from left to right: degraded image (VW-SSIM = 0.8881); Processed image using eq. (7), VW-SSIM = = 0.9767). Second line, from left to right: processed image using the symmetrical filter (VW-SSIM = = 0.9835), processed image using the asymmetrical filter (VW-SSIM = 0.9876).

The poorest result among the best 3 classified methods is obtained by the Tschumperlé-Deriche filter and it due to the fact that, despite being specifically designed to preserve curved structures, noise is filtered out only for large diffusion times inducing dissipative effects on edges. Our symmetrical filter performs significantly better in eliminating noise and limiting junction and corner modifications by slowing down or inverting deliberately the smoothing process in these regions. The better score obtained by the asymmetrical version of the filter is due to the fact that on asymmetric image patterns, by considering semi-differentiability on the positive sense of the diffusion axis, the filter's smoothing action is performed away from this type of discontinuities. On edges, the filter acts symmetrically and retains some parasite local minima of the luminance function due to noise; this is due to the formulation of the filter but we judge that the result is visually better, in correspondence with the quantitative indications.

The new filter can be applied whenever junction, corner and edge information preservation is important. Fig. 2 shows a comparative result obtained in ancient digital engraving restoration tasks. For the same set of parameters the proposed method better preserves relevant structures than its symmetric counterpart. Finally, in Fig. 3 we show comparative results between the proposed

method and non-PDE state-of-the-art methods in denoising the standard *fingerprint* image in an additive Gaussian noise scenario ($\sigma = 50$) [19].

Fig. 2 – Results on real images. From left to right: original image, image processed using the original formulation of the filter; image processed using the proposed method.

Fig. 3 – Results on denoising standard images. From left to right: BM3D [17] result (PSNR = 24.36 dB), BLS-GSM [18] result (PSNR = 23.29dB), result using eq. (9) (PSNR = 23.91dB).

Although the global PSNR value is higher for the BM3D method, by acting locally, our PDE retains better fine scale details and outperforms the BLS-GSM method. We observed the same behavior for this image on the whole range of Gaussian noise variances (σ^2) indicated in [19]; the mean PSNR value for BM3D is 27.70 dB, for BLS-GSM is 27.03 dB whilst for our method we obtained 27.16 dB. For BM3D and BLS-GSM we used the author's Matlab code with σ as parameter.

4. CONCLUSIONS

The paper proposes an efficient image restoration and enhancement approach based on the PDE framework and evolved orientation estimation techniques. The main novelty of the filter consists in considering asymmetric information in

characterizing and handling corners and junctions. We have shown that the new filter outperforms other classical and recent PDE methods. Further work will adapt the model for coping also with images composed of non-oriented patterns.

ACKNOWLEDGMENT

This work was funded by the PN2 CNCSIS-UEFISCSU ID_908/2007 grant.

Received on June 05, 2009

REFERENCES

1. P. Perona and J. Malik, *Scale space and edge detection using anisotropic diffusion*, IEEE Transactions on Pattern Analysis and Machine Intelligence, **12**, *7*, pp. 629-639 (1990).
2. F. Catte, P.L Lions, J.M. Morel, T. Coll, *Image selective smoothing and edge detection by nonlinear diffusion. I*, SIAM J. Numer. Anal., **29**, *1*, pp. 182-193 (1992).
3. J. Weickert, *Coherence enhancing diffusion*, International Journal of Computer Vision, **31**, *2*, pp. 111-127 (1999).
4. J. Weickert, *Coherence enhancing shock filters*, LNCS, **2781**, pp. 1-8 (2003).
5. R. Terebes, O. Lavialle, M. Borda, P. Baylou, *Flow Coherence Diffusion. Linear and Nonlinear Case*, Lecture Notes in Computer Science, **3708**, pp. 316-322 (2005).
6. R. Carmona, S. Zhang, *Adaptive smoothing respecting feature directions*, IEEE Transactions on Image Processing, **7**, ***3***, pp. 353-358 (1998).
7. D. Tschumperlé, *Fast Anisotropic Smoothing of Multi-Valued Images using Curvature-Preserving PDE's*, International Journal of Computer Vision, **68**, *1*, pp. 65-82 (2006).
8. D. Tschumperlé, *LIC-Based regularisation of multi-valued images*, IEEE International Conference on Image Processing, **3**, pp. 533-536. Genoa, Italy, September 2005.
9. D. Tschumperlé, R. Deriche, *Vector-valued image regularization with PDE's*, IEEE Transactions on Pattern Analysis and Machine Intelligence, **27**, *4*, pp. 506-517 (2005).
10. R. Terebes, M. Borda, B. Yuan, O. Lavialle, P. Baylou, *A new PDE bassed approach for image restoration and enhancement using robust diffusion directions and directional derivatives based diffusivities*, The 7th IEEE International Conference on Signal Processing ICSP2004, Beijing, China, pp. 707-712, Aug. 31-Sept. 4 (2004).
11. S. Arseneau J. Cooperstock, *An asymmetrical diffusion framework for junction analysis*, British Machine Vision Conference, (BMVC 2006), **2**, pp. 689-698, Edinburgh (2006).
12. F. Michelet, J.P. Da Costa, O. Lavialle, Y Berthoumieu, Pierre Baylou C. Germain, *Estimating local multiple orientations*, Signal Processing, **87**, *7*, pp. 1655-1669 (2007).
13. R. Terebes, M. Borda, C. Germain, O. Lavialle, S. Pop, *Asymmetric directional diffusion based image filtering and enhancement*, International Conference on Automation, Quality and Testing, Robotics AQTR2008, **3**, pp. 413-416 (2008).
14. W.J. Connover, R.L. Imam, *Rank transformations as a bridge between parametric and nonparametric Statistics*, The American Statistician, **35**, pp. 124-129 (1981).
15. A.C. Bovik, J. Gibson, *Handbook of image and video processing*, Elsevier, 2005, pp. 967-970.
16. G. Aubert, P. Kornprobst, *Mathematical problems in image processing. Partial Differential Equations and the calculus of variations*, Springer, 2006, pp. 323-337.
17. V.A. Katkovnik,. K. Foi, K. Egiazarian, J. Astola, *From local kernel to nonlocal multiple-model image denoising*, Int. J. Computer Vision, **86**, *1*, pp. 1-32 (2010).
18. J.Portilla, V. Strela, M Wainwright, E.P. Simoncelli, *Image Denoising using Scale Mixtures of Gaussians in the Wavelet Domain*, IEEE Trans. on Image Process, **12**, *11* pp. 1338-1351 (2003).
19. ***, http://www.cs.tut.fi/~foi/GCF-BM3D/ – *Block-matching and 3D filtering (BM3D) algorithm*